Estimation of nocturnal CO_2 and N_2O soil emissions from changes in surface boundary layer mass storage

Richard H. Grant[1], Rex A. Omonode[1]

[1] Department of Agronomy, Purdue University, West Lafayette, Indiana, 47907, USA

Correspondence to: Richard H. Grant (rgrant@purdue.edu)

Abstract. Annual emissions of greenhouse and other trace gases requires knowledge of the emissions throughout the year. Unfortunately emissions into the surface boundary layer during stable, calm nocturnal periods are not measureable using most micrometeorological methods due to non-stationarity and uncoupled flow. However, during nocturnal periods with very light winds carbon dioxide (CO_2) and nitrous oxide (N_2O) frequently accumulates near the surface and this mass accumulation can be used to determine emissions. Gas concentrations were measured at four heights (one within and three above canopy) and turbulence was measured at three heights above a mature 2.5 m high maize canopy from 23 July to 10 September 2015. Nocturnal CO_2 and N_2O fluxes from the canopy were determined using the accumulation of mass within a 6.3 m vertical domain of the nocturnal surface boundary layer. Diffusive fluxes out of the top of this domain were also estimated. Fluxes during near-calm nights (friction velocities < 0.05 ms^{-1}) averaged 906 mg CO_2 m^{-2} h^{-1} and 38 μg N_2O m^{-2} h^{-1}. Fluxes were also measured using chambers during corresponding days. Carbon dioxide flux determined by the accumulation method were generally comparable to those determined using soil chambers. Nitrous oxide flux determined by the accumulation method were equal to or below those determined using soil chambers. The more homogenous emission of CO_2 over N_2O from nearby fields and the better signal to noise ratio of the chamber method for CO_2 over N_2O were likely major reasons for the differences in chambers versus accumulated nocturnal mass flux estimates. Near-surface N_2O accumulation flux measurements in more homogeneous regions and with greater depth are needed to confirm the conclusion that mass accumulation can be effectively used to estimate soil emissions during nearly calm nights.

1 Introduction

Evaluation of the annual emissions of greenhouse and other trace gases emitted from agricultural fields and landscapes requires knowledge of the emissions during representative periods of the year. Micrometeorological methods are widely used to evaluate the emissions and uptake of carbon dioxide (CO_2) and to a lesser degree nitrous oxide (N_2O). The micrometeorological methods of integrated horizontal mass flux, eddy covariance, eddy diffusion, or Eulerian or Lagrangian dispersion however cannot be used to determine the exchange during stable, calm nocturnal periods due to turbulence characteristics assumptions (Pattey, et al, 2002). Various efforts to estimate the exchange during these periods have been devised- in some cases using purely statistical methods, some using empirical relationships, and some using alternative flux measurement methodologies

(Aubinet et al, 2012). The primary difficulties of determining the flux in the surface boundary layer under stable nocturnal conditions include the possibility of advection, non-stationarity of the concentration and velocity fields, and the lack of a similarity theory to describe the non-stationary, intermittent exchange processes. A result of the negligible turbulent transport of mass away from the surface is a temporal change in storage of mass within a layer near the surface primarily a result of low vertical turbulent diffusion. This accumulation occurs initially in a shallow nocturnal surface boundary layer then through light continuous or intermittent turbulence deepens through a thicker (on the order of 100 m) stable nocturnal boundary layer (Kaimal and Finnigan, 1994). Xia et al (2011) noted an accumulation of ^{222}Rn within a 6.5 m surface boundary layer over a grass clearing of a forest preserve during nights with clear sky, light winds, and strong radiative cooling. Similar gas accumulations in the surface boundary layer at night have been conducted for CO_2, CH_4, and N_2O over pastures and crops (Pattey et al, 2002; Pendall et al., 2010). As weak turbulence mixes the surface boundary layer air with the cooling stable nocturnal boundary layer, gas mass accumulations become evident throughout much of the stable nocturnal boundary layer. Such mass accumulations are reported for CO_2, CH_4, and N_2O over crops, plantations, and forests (Pattey et al, 2002; Acevedo, et al., 2004; Acevedo, et al., 2008).

Weak turbulence and stable conditions prevent effective use of flux footprint estimates (Vesala et al, 2008). Hence regional-scale horizontal heterogeneity of soil-emitted gasses introduces significant potential for advection under these conditions. This advection component to the measured mass accumulation cannot be readily assessed since the determination of flux footprints depends on turbulent mixing (Vesala, 2008). Chambers et al (2011) attempted to determine the relative contribution of Rn accumulation from mixing of local sources and that advected from 'remote' regions with greater or less soil flux.

Using temporal mass accumulation for estimating flux under stable conditions assumes horizontal transport is negligible, there are no local sources of N_2O or CO_2 within the control volume, and that the exchange of mass between the control volume and the overlying air is minimal. If there is no flow in the surface boundary layer (SBL), then gases emitted from the soil surface will diffuse upward at roughly the rate of molecular diffusion (approx. 10^{-5} m^2s^{-1}). Compared to the typical turbulent diffusion exchange coefficients, the molecular diffusion rate is negligible. Consequently gas diffusion from the surface is effectively stopped at any altitude were the diffusion rate approaches the molecular rate. This provides the effective 'cap' on the mixing of gases in the control volume layer.

Many definitions have been used to define the conditions in which the accumulation of a gas as effectively capped in the surface boundary layer. Since the friction velocity (u_*) provides an index of turbulent mixing, Pattey et al (2002) used a u_* threshold for validating the quality of the 'cap'. Pendall et al (2010) defined the top of the control volume based on significant correlations between CO_2 (presumed from soil respiration) and CO, CH_4, N_2O, and H_2. The top of the control volume has been estimated by Acevedo et al (2004) using the top of an observed fog layer or the height of constant potential temperature and specific moisture between 0530 and 0830 LT. Acevedo et al (2008) used the height of the strongest potential temperature inversion as the control volume top. Pattey et al (2002) determined the accumulation over the entire 10 m of profile measurements under constrained turbulent flow conditions. Using these 'cap' definitions, the temporal change in mass

accumulations have been determined over relatively thin layers of air over crops (10 m thick; Pattey et al, 2002), pastures (5 m thick; Pendall et al., 2010) and plantations (8 m thick; Pendall et al., 2010). Other much thicker layers of at least 20 m have been defined over forests (Acevedo, et al., 2004; Acevedo, et al., 2008; Pendall et al., 2010).

We evaluated the nocturnal flux of CO_2 and N_2O from maize-cropped land based on the temporal accumulation of mass storage within the surface boundary layer constrained vertically by the flow characteristics at the top of the layer.

2 Methods

N_2O and CO_2 fluxes were measured using three methods during the night between 2000 and 0400 local time (LT) over nitrogen-fertilized fields during the summer of 2015. These fields are located in a relatively flat and homogeneous terrain (Fig. 1a) near West Lafayette, Indiana, USA (40.495° latitude and -86.994 ° longitude). The terrain rises to the north at a rate of only 2 m km^{-1} and land use is predominantly agricultural with cropped land covering 100% of the land within 1 km^2 and 97% of the within 10 km^2 (Table 1) and 83% within 25 km^2. Crops are generally alternating between maize and soybean with 83%, (1 km^2) 46% (10 km^2) and 40% (25 km^2) in maize in 2015.

The instrumented tower (described below) was situated in a tilled field (Fig. 1b) in which 200 kg N ha^{-1} were applied as anhydrous ammonia (AA) at pre-plant in spring 2015. Three other fertilizer treatments were applied in fields near the tower: a fall 200 kg N ha^{-1} AA application on a till field to the east during the fall of 2014, a 100 kg N ha^{-1} AA on a no-tilled field to the southeast during the fall of 2014 followed by a pre-plant spring AA application of 100 kg N ha^{-1} on a tilled and no-till field, and a spring pre-plant application of 200 kg/ha N on a field directly south.

N_2O and CO_2 concentrations were measured from air sampled out of a 7 L min^{-1} air flow drawn from 1μm-filtered inlets at three heights: 2.8 m, 5 m, and 8 m above ground level (agl). Air was sampled sequentially for 5 minutes at each inlet. Mean concentrations were based on the last three of each five-minute interval to account for the time lag associated with the air flow and the measuring instruments. The 2.8 m point sample was made from a mast that was 18 m from the 5 and 8 m measurement mast (Fig. 1b). In addition a line sample based on a 50-m line with ten inlets drew air at 1 m within the canopy (Grant and Boehm, 2015). The 1 m in-canopy line sample measurement was positioned between 50 m and 25 m (line sample end to end) from the 5 m and 8 m single point mast measurements (Fig. 1b). The 2.8 m single point measurement was made between 45 m and 65 m from the 1-m line sample (end to end) and 18 m from the 5 and 8 m measurement mast (Fig. 1b). The N_2O in the sampled air was measured using an IRIS 4600 difference frequency generation (DFG) laser mid-infrared (IR) analyzer (ThermoFischer Scientific, Franklin, MA) with a measured N_2O minimum detection limit (MDL; 3 sigma) of 0.3 nLL^{-1}. The CO_2 in the sampled air was measured using a LiCOR 840 non-dispersive IR analyzer (LiCOR, Inc., Lincoln, NE) with a measured CO_2 MDL of 5 μLL^{-1}. The moisture content of the sampled air was also determined by the LiCOR 840 non-dispersive IR analyzer. All concentrations were corrected to dry air.

Atmospheric pressure, temperature and relative humidity were measured at 2.5 m at 5-min intervals on a weather station within 100 m of the gas measurements. Turbulence was measured at three heights (2.5 m, 5 m, and 8 m) using a 3-dimensional sonic anemometer (RM Young 81000, RM Young, Inc., Traverse City, MI). Turbulence was sampled at 16Hz and recorded at 10Hz. The minimum detection limit (MDL) was approximately 0.01 ms^{-1}. Since the tethered tower was tilted but shifted slightly in tilt due to shifts in the wind direction, a double rotation rather than planar rotation was made to correct the flow coordinate system for each 30-min turbulence-averaging interval (Lee et al, 2004). Stability was assessed using the local Obukhov length (Λ) based on local measures of heat and momentum transfer within the stable boundary layer (van de Wiel et al, 2008).

The accumulation of CO_2 and N_2O over the maize canopy was based on gas concentration measurements (using the DFG and NDIR instruments) made at three heights (3m, 5m and 8m; Fig. 1b) on an 8m tower and one height representing an integrated line concentration in the maize canopy (1 m; Fig. 1b). Flux was determined into the layer according to:

$$Q_C = \frac{\Delta \int_0^{6.3} C dz}{\Delta t} \quad (1)$$

using Newtonian integration and assuming the concentration between the ground and 1 m was constant and equal to that at 1 m . The accumulation flux was calculated as the linear slope of the time resolved accumulation of three measurements over 1.5 hours. Turbulent conditions were segregated into those with u_* less than or greater than or equal to 0.05 ms^{-1} (approximately four times the estimated MDL of 0.014 ms^{-1}). This threshold was lower than that used by Pattey et al (2002), who used a threshold of 0.1 ms^{-1} for both the friction velocity (u_*) and standard deviation of w (σ_w).

The diffusive flux out the top of the control volume (6.3 m) under both unstable and stable conditions was determined using the eddy exchange coefficient K_c as:

$$Q_C = K_C \frac{\Delta C}{\Delta z} \quad (2)$$

where the concentration gradient ($\Delta C/\Delta z$) was calculated above the canopy between 5 m and 8 m (van de Wiel et al, 2008). The ΔC MDL were estimated at 12.7 μLL^{-1} for CO_2 and 0.5 nLL^{-1} for N_2O based on the MDL for the respective gas concentrations. The K_c for top of the control volume was determined using 3D sonic anemometer measurements at 5m and 8m using the similarity method of Schaefer et al. (2012) and the molecular Schmidt number (0.91 for CO_2 and 0.95 for N_2O; Massman, 1998). Given the sonic anemometer measurement error in wind speed and the corresponding error in friction velocity, the error in K_c was estimated at 22%, or approximately 0.0035 m^2s^{-1}. Diffusive fluxes where the ΔC or K_c were less than the MDL were invalidated. Since the double rotation coordinate tilt induce additional errors in u_* for u_* less than 0.15 ms^{-1} (Foken et al, 2004), the error in K_c was expected to be much lager for low turbulence conditions.

The CO_2 and N_2O emissions were also determined using the vented static chamber method at various times between 1000 and 1400 LT over the two months of measurements (Mosier et al, 2006). Diurnal variation in chamber N_2O emissions were

assessed over four days in August (5-8 August 2015) with measurements at 00, 06, 12, and 18 h LT. The chamber consisted of aluminium anchors (~0.74 by 0.35 by 0.12 m) driven about 0.10 m into the soil; at each sampling time lids covered the anchors to result in a chamber volume of approximately 32.4 L. On each sampling date, gas samples were collected from the chamber headspace through a rubber septum at 0, 10, 20, and 30 min after chamber deployment using a gastight syringe, and then transferred into pre-evacuated 12 mL Exetainer vials (Labco, High Wycombe, UK). Nitrous oxide and CO_2 concentrations of the gas samples were determined using a gas chromatograph (Varian 3800 GC, Mississauga, Canada) equipped with an automatic Combi-Pal injection system (Varian, Mississauga, Canada). Fluxes were calculated from the rate of change of the N_2O concentration in the chamber headspace assuming a linear rate of change in concentration within the headspace. The MDL determined based on the 99% confidence interval of the rate of change was 3.7 nmol $m^{-2}s^{-1}$ for CO_2 flux and 0.7 nmol $m^{-2}s^{-1}$ for N_2O.

Comparisons between the chamber method and mass accumulation method flux were made over three time intervals: 23 to 31 July, 1 to 22 August, and 23 August to 2 September. Statistics of all chamber measurements were made regardless of field measured. Statistics of mass accumulation measurements were made regardless of the time of day of measurement. Student's t-test was used to determine if there was a significant difference at p=0.05 between the chamber and mass accumulation measurements.

Land use during the 2015 growing season was assessed using CropScape Cropland Data Layer (USDA,2017). Dominant land use, excluding developed land, was assessed for the surrounding 1 km^2 and 10 km^2 area of the measurement tower (Table 1).

3 Results and Discussion

Measurements were made over the period 23 July to 11 September, 2015 resulting in 1685 30-min averaged records. Within this period there were 600 ½ h periods with N_2O measurements and 370 30-min periods with CO_2 measurements between 1900 and 0300 LT. During this period, the mature maize canopy was 2.5 m tall (H).

3.1 Near-surface layer profiles

A common feature of the nocturnal CO_2 and N_2O concentration profiles is an increase in concentration near the surface over time (Fig. 2b,c). Mass accumulations of CO_2 and N_2O were observed over the mature maize canopy when wind speeds were low at 8 m (3.2H) (Fig. 2a). The increased concentrations were assumed to be a result of gaseous emissions largely from the soil surface. Mean wind speed (U) and the ratio of variability in w (σ_w) to u_* at both 5 m and 8 m were significantly lower when $u_* < 0.05$ ms^{-1} than when $u_* > 0.05$ ms^{-1} (Table 2; Fig. 3). Over the nocturnal period of 1900 to 0700 LT, the averaged local stability at 8 m (z/Λ; van de Wiel et al, 2008) at 8 m was positive regardless of u_* between 1900 and 0300 LT and negative from 0300 and 0700 LT. The negative stability expressed the influence of dawn occurring around 05 LT (Table 2). Stable conditions (positive Λ) at 8 m occurred during 28% of the measurement periods (465 30-min measurement intervals).

Sonic temperature (T_s) increased with height between 3 and 5 m under low turbulent conditions throughout the night while increasing turbulence between 20 and 0700 LT shifted the T_s gradient from positive to negative with height (Fig. 2). However at the top of the measured profile, the temperature gradient was nearly zero for $u_* < 0.05$ ms^{-1} (Table 3). The mean bulk Richardson number (R_B) at the geometric mean height of the top two measurements averaged 2.3 when $u_* < 0.05$ ms^{-1}. For conditions with $u_* >= 0.05$ ms^{-1} the mean R_B was -1.2. Shifts in wind direction above the canopy (5 to 8 m height) were highly variable for u_* less than approximately 0.05 ms^{-1} (Fig. 3). These shifts coincided with vertical wind velocity variance less than 0.01 m^{2}s^{-2} and the horizontal wind velocity variance less than 0.1 m^{2}s^{-2} (Fig. 3). At these low turbulence conditions, turbulent transport of gases originating at the earth surface is minimal resulting in the accumulation of gases in a layer of air bounded by a 'cap' in the surface boundary layer. The top of the surface-influenced domain in which mass accumulation was set at 6.3 m (geometric mean of 5 m and 8 m; 2.5H) (Fig. 4).

Over the 1900 to 0700 LT timeframe, the line-averaged concentrations of CO_2 at 1 m within the canopy ranged from 354 μLL^{-1} to 1038 μLL^{-1} while point concentrations at 8 m agl (5.2 m or 2.9 H above the canopy) varied from 358 μLL^{-1} to 862 μLL^{-1}. The difference between the 5 m (1.7 H) and 8 m (2.9H) CO_2 concentrations ranged from -11.4 μLL^{-1} to 337 μLL^{-1}. Given the MDL of a delta concentration of 12.7 μLL^{-1} CO_2, the MDL of the gradient at the top of the domain was 7.8 mg CO_2 m^{-4}. Approximately 22.7% of the concentration gradients at the top of the layer were high enough to calculate a turbulent diffusion. The mean CO_2 gradient ($\Delta CO_2/\Delta z$) was less than or equal to the MDL when $u_* > 0.05$ ms^{-1} (Table 3).

Over the1900 to 0700 LT timeframe, the line-averaged N_2O concentrations within the canopy (0.4H) ranged from 0.313 μLL^{-1} to 0.467 μLL^{-1} while the point sample at 8 m ranged from 0.295 μLL^{-1} to 0.448 μLL^{-1}. The difference between the 5 m (1.7 H) and 8 m (2.9H) N_2O concentrations above the canopy ranged from -0.357 μLL^{-1} to 0.059 μLL^{-1}. Given the MDL of a delta concentration of 0.5 μLL^{-1} N_2O, the MDL gradient at the top of the domain was 0.307 μg N_2O m^{-4}. Only 0.2% of the concentration gradients at the top of the layer were high enough to calculate a turbulent diffusion. The mean N_2O gradient ($\Delta N_2O/\Delta z$) was less than the MDL when $u_* > 0.05$ ms^{-1} (Table 3).

A common feature of the mean concentration profiles of both CO_2 and N_2O was a lower mean concentration from air sampled at a point 3 m (1.2H) than both the 1 m (0.4H) and 5 m (1.7H) mean concentrations. This may be a result of the close proximity of the 1.2 H point measurement to the canopy top representing only local canopy conditions. Conversely, the spatially-averaged line concentration in the canopy at 0.4H could better approximate the mean concentration at that height within the canopy. Consequently, concentration measurements at 2.8 m were excluded from all profiles prior to mass integration.

The pattern of mass build-up were similar for N_2O and CO_2 (Fig. 4). The increase in either N_2O or CO_2 concentrations in the lowest 6.3 m corresponded with a decrease in wind speeds at 8 m (Fig. 2) as well as low u* and variance in w (Fig. 4). The mean gradient in N_2O and CO_2 at this height during stable conditions and low turbulence was higher than that during higher turbulence, although the gradients varied widely (Table 3). If winds intermittently increase during the night, the concentration of both N_2O and CO_2 decreased in the surface boundary layer, with an increase occurring after the winds decline again (Figs.

1, 3). This intermittent turbulence then mixed the heat and mass further into the developing nocturnal boundary layer. The accumulation of CO_2 and N_2O in the lowest 8 m of the boundary layer might be expected to occur if the top of the layer exhibited minimal turbulence since the molecular diffusion of a gas is orders of magnitude smaller than the turbulent diffusion.

On average, the mean profiles of CO_2 and N_2O concentrations during from 1900 to 0300 LT showed nearly identical concentrations at 1 m and 5 m with decrease in concentration at 8 m (Fig. 5). The corresponding mean concentration profiles for the 0300 to 0700 LT time window showed no change in concentration with height (Fig. 5). Conditions during the 1900 to 0300 LT period resulted in nearly identical mean wind speed profiles regardless of u_* but substantially different temperature profiles (Fig. 5). Temperature inversions above the canopy (2.8 m to 5 m agl) were evident between 1900 and 0300 LT regardless of u_* (Fig. 5). The temperature inversion was also evident between 0300 and 0700 LT when u_* was less than 0.05 ms^{-1} (Fig. 5). This near-surface inversion was not evident at the top of the accumulation domain (between 5 m and 8 m agl) where the wind shear was high.

3.2 Mass accumulations

Using the previously defined top of the accumulation domain, the accumulations of N_2O and CO_2 were often evident during the night from 1900 to 0000 LT with sunset approximately 2100 LT (Fig. 6). These mass accumulations corresponded with positive z/Λ (locally stable conditions) and low u_* (low turbulence). After quality assurance of the accumulated flux calculations, there were 90 30-min measurements of N_2O nocturnal flux and 85 30-min measurements of CO_2 nocturnal flux with u_* less than 0.05 ms^{-1}. Note that the mean gradients of both N_2O and CO_2 were less for this set of measurements (Table 4) than for all measurement periods (Table 3). Accumulated N_2O flux during low turbulence averaged 0.38 □□□□ $m^{-2}s^{-1}$ with a variability (standard deviation) greater than the mean (Table 4). Mean accumulation N_2O fluxes late in the growing season were comparable both to the median flux measured over many months using K_{N2O} over maize by Wagner-Riddle et al (2007) and fluxes measured using chambers by Venterea and coworkers (2005). The accumulation CO_2 flux during low turbulence averaged 4.1 μmol $m^{-2}s^{-1}$ with a variability less than the mean (Table 4). These fluxes are comparable to those reported by Mosier et al (2006) over a maize field.

Greater turbulence (higher u_* at 8 m) corresponded with decreased accumulated fluxes for both N_2O and CO_2 (Table 4). The greater turbulence corresponded with a decrease in the mean N_2O gradient and an increase in the CO_2 gradient at the top of the domain (Table 4). The mean NO_2 flux and mean N_2O gradients both decreased with increased u_* (Table 4). The upper transport 'cap' to the mass accumulation domain was on average stronger for the low turbulence condition than the higher turbulence condition (based on σ_w and σ_w/u_*; Table 2). The effectiveness of this 'cap', separating the developing nocturnal boundary layer above from the surface boundary layer below, had a larger effect on the mass accumulation of N_2O than CO_2. This might be expected if the local CO_2 flux was more similar to the more distant surroundings (more homogeneous) than the N_2O flux. It is important however to note that the high variability in CO_2 and N_2O fluxes under low turbulence resulted in a mean flux not statistically different (Student t-test) from that associated with turbulence with u_* up to 0.05 ms^{-1} (Table 4).

Eddy diffusivities were comparable to and exhibited the same relationship to u_* and z/Λ for positive z/Λ as those reported for N_2O and NH_3 in Schaefer et al. (2012). The mean eddy diffusivities were more than an order of magnitude higher for conditions with $u_* > 0.05$ ms^{-1} than $u_* < 0.05$ ms^{-1} (Table 3). Clearly the u_* threshold of 0.05 ms^{-1} still allowed for weak turbulent diffusion of the both N_2O and CO_2 out of the near-surface control volume and into the nocturnal boundary layer (Table 4). Measureable upward turbulent diffusive transport was evident for 44% of the accumulated N_2O flux measurements and 33% of the accumulated CO_2 flux measurements during the 1900 to 0300 LT time window (Table 4). Excluding intervals when the diffusive flux was measureable reduced the low turbulence flux of N_2O mean flux to 0.27 □□□□m^{-2}s^{-1} and slightly increased the CO_2 mean flux to 4.2 μmol m^{-2}s^{-1} (Table 4), although these differences were not statistically different from the fluxes during periods with measurable diffusive flux. When turbulence at 8 m exceeded u_* of 0.05 ms^{-1}, the accumulation flux of N_2O was approximately 15% lower than that under low turbulence while that of CO_2 was more than 50% lower (Table 4). However if there is z-less flow (Marht, 2011) at the domain top at low u_*, the applicability of diffusion estimates using Equation 2 across the top of this domain is questionable. An alternate explanation of the relatively small changes in flux of both N_2O and CO_2 at low u_* with or without estimated diffusion (Table 4) is a lack of applicability of the approach to estimating diffusion.

The time trends in the mass accumulation fluxes of N_2O and CO_2 when there was no measurable diffusive flux are illustrated in Figures 6 and 7. The accumulated fluxes of CO_2 between 1900 LT and 0300 LT generally decreased over time with values ranging from approximately 2.0 to 0.2 μmol m^{-2}s^{-1} (Fig. 7). Consequently, the standard deviation of the mean flux of 2.7 μmol m^{-2}s^{-1} does not represent the variability in flux as much as the mean trend over time. Additional measurements when there was no measurable diffusive flux between 0300 LT and 0700 LT were similar to those during the night (small filled circles, Fig. 7).

The accumulated fluxes of N_2O were relatively steady over the measurement period (Fig. 8). Since the MDL for the flux estimate was much smaller than these fluxes, the standard deviation of 0.4 nmol m^{-2}s^{-1} (Table 4) appears to represent the variability in flux associated with varying winds during the night. Additional measurements when there was no measurable diffusive flux between 0300 LT and 0700 LT were slightly higher than those during the night (Fig. 8).

3.3 Soil chamber fluxes

The daytime (between 1000 LT and 1400 LT) soil chamber CO_2 and N_2O flux measurements made during the measurement period also showed a decreasing flux over the period (Figs. 6, 7). CO_2 flux ranged from 0.1 μmol m^{-2}s^{-1} to 2.1 μmol m^{-2}s^{-1} and averaged 0.9 μmol m^{-2}s^{-1}. These chamber measurements had a mean signal to noise ratio of 250. These fluxes are similar to soil+root respiration fluxes reported in the literature for maize fields (Table 1). The region of the south field in which no N was applied during the past year had a mean CO_2 emission of 0.5 μmol m^{-2}s^{-1}, averaging 50% of the mean field emissions under various N treatments and similar to that reported for soil+root respiration of soybean in the literature (Table 1). The four-day study of diurnal variation in mean hourly CO_2 emissions ranged from 1.04 μmol m^{-2}s^{-1} to 1.48 μmol m^{-2}s^{-1} with the highest emissions at 1800 LT with a ratio of midnight to noon LT emissions of 1.2.

Nitrous oxide fluxes ranged from 0.3 nmol $m^{-2}s^{-1}$ to 2.2 nmol $m^{-2}s^{-1}$ averaging 1.1 nmol $m^{-2}s^{-1}$. These fluxes were lower than commonly reported in the literature for maize but similar to that of soybeans (Table 1). This may be due to the negligible amount of the applied nitrogen available for denitrification and nitrification in the maize field. These chamber N_2O measurements thus had a mean signal to noise ratio of 1.7. The field south of the tower, on which no N was applied during the year, had a mean emission of 0.59 nmol $m^{-2}s^{-1}$, 54% of the mean fertilized field emissions and equal to the Chamber method MDL. The four-day study of diurnal variation in mean hourly N_2O emissions ranged from 0.96 nmol $m^{-2}s^{-1}$ to 1.40 nmol $m^{-2}s^{-1}$ with the highest emissions at 1800 LT with a ratio of midnight to noon LT emissions of 0.93.

3.3 Comparative fluxes

As with the comparison of CO_2 fluxes determined by eddy covariance and boundary-layer mass balance (Eugster and Siegrist, 2000), the fluxes determined by chamber and mass accumulation are local and 'regional' fluxes respectively. The CO_2 flux measurements based on mass accumulation within the domain during low turbulence and stable conditions were comparable to the chamber measurements with a few outlier high mass accumulation values (Fig. 7). Although in the days in which chamber and mass accumulation fluxes were made the two fluxes were comparable (Fig 7), the mean period fluxes over two of the three measurement time periods indicated the mass accumulation method flux was only 0.6 to 0.9 of that determined by the chamber method (Table 5). Higher accumulation flux over the chamber flux was expected due to the chamber flux method measured only root and soil respiration while the mass accumulation flux method measured the respiration of the soil, roots, stalks and leaves. This can result in a large difference in flux: Parkin et al (2005) measured soil and root respiration with chambers and whole canopy respiration by eddy covariance and found that the soil respiration was approximately 50% of the total measured CO_2 flux. The chamber and mass accumulation fluxes were not significantly different given the variability in chamber fluxes over each of the three measurement periods (Table 5).

The N_2O flux measurements based on mass accumulation under low turbulence and stable conditions were generally lower than those measured using the chambers on the same day (Fig. 8). However when comparing the mean period fluxes over the three measurement time periods, the mean mass accumulation method fluxes ranged from 0.5 to 1.1 times those determined by the chamber method (Table 5). Since there is no known N_2O flux from the crop canopy, the soil chamber flux should be the same as the above-canopy accumulation flux provided there is no advection of low N_2O air from nearby. However, the higher chamber fluxes might be anticipated since the chamber fluxes were measured during the daytime when soil temperatures were higher. However, the diurnal chamber flux measurements showed only slightly lower fluxes during the daytime than night (factor of 0.93). The chamber and mass accumulation fluxes were not significantly different given the variability in chamber fluxes over each of the three measurement periods (Table 5).

The accumulated mass of CO_2 and N_2O have contributions from local soils sources as well as mass advection from more distant sources due to the meandering nature of the air flow during the stable nocturnal conditions (Eugister and Siegrist, 2000). Unfortunately, the analytical approaches to defining the flux footprint do not apply to the stable nocturnal conditions in which

the accumulations occur ($z/\Lambda>+1$, $u_* < 0.05$ ms^{-1}); Vesala et al, 2007), although they are believed to be in the order of kilometers (eg. Chambers et al, 2011). At scales of kilometers, the land use was crop agriculture; dominated by soybean and maize production (93%) in the 10 km^2 area of the measurement tower (Table 1).

Differences between the accumulation flux versus chamber flux measurements were likely in part due to the advection of gas emitted from surrounding fields. The CO_2 emissions of the un-fertilized fields were similar to those of the fertilized fields (Fig. 7) and literature values for emissions from surrounding grassy areas and soybean fields are similar to these emission rates (Table 1), it is reasonable to assume that the advected, regionally-emitted CO_2 from surrounding soybean and maize production would not be evident in our measurements.

The measured un-fertilized fields of maize typically had lower N_2O emissions than fertilized maize fields, closer emission rates to those measured by the accumulation method (Fig. 8). Literature values for emissions from surrounding grassy areas and soybean fields are substantially lower than the measured fertilized maize fields (Table 1). Since roughly one-half the surrounding area was in soybean production (Table 1), it is reasonable to assume horizontal advection of air with lower N_2O concentration from nearby soybean canopies likely affected the N_2O profile. This advection would be expected to decrease the mass accumulation since the N_2O fluxes from soybean less than of maize (Table 1). Additional measurements when there was no measurable diffusive flux between 0300 LT and 0700 LT suggest that the accumulated fluxes were comparable to those of the chamber measurement method (Fig. 8). These flux measurements were bounded at the top of the domain by slightly unstable conditions (Table 2).

The underestimate of CO_2 and N_2O fluxes using the mass accumulation method may be a result of using two small of a accumulation volume. The 'cap' of the volume was arbitrarily set at the geometric mean between the upper two measurement heights. An objective measure of the 'cap' height is needed.

4 Conclusions

Nocturnal CO_2 and N_2O fluxes from the soil surface were determined using the accumulation of mass within a mixing-limited surface boundary layer domain. The accumulation flux estimation required the friction velocity near the confined domain top to be less than 0.05 ms^{-1}, with or without intermittent turbulence, to assure limited turbulent diffusion out the domain top and into the deeper nocturnal boundary layer.

The surface flux determined by the accumulation method were similar to or less than fluxes measured using the vented static chamber method under these near-calm stable conditions. The magnitude and homogeneity of the flux influenced the ability for the accumulation method to be effective at estimating nocturnal flux: CO_2 flux determined by the accumulation method were comparable to those measured using the chamber method while that for N_2O was at or below that measured using the chamber method. For the N_2O flux, there is no known canopy emission of N_2O and consequently the chamber method and accumulation method should have been comparable. Advection of air during the stable nocturnal conditions contributed to the measured profiles and likely resulted in underestimation of the N_2O flux, but not the CO_2 flux, by the accumulation method.

Additional work is needed to evaluate the use of the accumulation method for N_2O fluxes for accumulations within a larger vertical domain and more homogeneous horizontal domain using chamber methods with a lower MDL (higher signal to noise ratio).

Author Contribution

R. Grant designed, conducted and analysed the mass accumulation experiment while R. Omonode conducted the chamber gas flux measurements. R. Grant prepared the manuscript with contributions from R. Omonode.

Competing interests

The authors declare that they have no conflict of interest.

Acknowledgements

The authors appreciate the field technical assistance of Cheng Hsien Lin and Austin Pearson.

References

Acevedo, O.C., Moraes, O.L., DaSilva, R., Fitzjarrald, D.R., Sakai, R.K., Staebler, R.M. and Czikowsky, M.J.: Inferring nocturnal surface fluxes from vertical profiles of scalers in an Amazon pasture. Global Change Biology 10, 886-894, 2004.

Acevedo, O.C., DaSilva, R., Fitzjarrald, D.R., Moraes, O.L., Sakai, R.K. and Czikowsky, M.J.: Nocturnal vertical CO2 accumulation in two Amazonian ecosystems. J. Geophy. Res. 113, G00b004, doi:10.1029/2007JG000612, 2008.

Aubinet, M., Feigenwinter, C., Heinesch, B., Laffineur, Q., Papale, D., Reichstein, M., Rinne, J. and van Gorsel, E.: Chapter 5: Nightime flux correction, In: Aubinet, M., Vesala, T. and Paple, D. (eds) Eddy Covariance: A Practical Guide to Measurements and Data Analysis. Springer Atmospheric Sciences, doi 10.1007/978-94-007-2351-1_5, pp 133-172, 2012.

Bowden, R.D., Rullo, G., Stevens, G.R. and Steudler, P.A.: Soil fluxes of carbon dioxide, nitrous oxide and methane at a productive temperate deciduous forest. J. Environ. Qual. 29, 268-276, 2000.

Bremner, J.M., Breitenbeck, G.A. and Blackmer, A.M.: Effect of anhydrous ammonia fertilization on emission of nitrous oxide from soils. J. Environ. Qual.10, 77-80, 1981.

Bremner, J.M., Robbins, S.G. and Blackmer, A.M.: Seasonal variability in emissions of nitrous oxide from soil. Geophys. Res. Lett. 7, 641-644, 1980.

Chamber, S., Williams, A.G., Zahorowski, W., Griffiths, A. and Crawford, J.: Separating remote fetch a local mixing influences on vertical radon measurements in the lower atmosphere. Tellus 63B, 843-859, 2011.

De Costa, J.M.N., Rosenberg, N.J., and Verma, S.B.: Respiratory release of CO2 in alfalfa and soybean under field conditions. Agric. Forest Meteorol. 37, 143-158, 1986.

De Jong, E., Schappert, H.J.V. and McDonald, K.B.: Carbon dioxide evolution from virgin and cultivated soil as affected by management practices and climate. Ca. J. Soil Sci. 54, 299-307, 1974.

Duxbury, J.M. and Bouldin, D.R.: Emissions of nitrous oxide from soils. Nature (London) 298, 462-262, 1982.

Eichner, M.J.: Nitrous oxide emissions from fertilized soils: summary of available data. J. Environ. Qual. 19, 272-280, 1990.

Eugster, W. and Siegrist, F.: The influence of nocturnal CO_2 advection on CO_2 flux measurements. Basic Appl. Ecol. 1,177-188, 2000.

Foken, T., Goeckede, M., Mauder, M., Mahrt, L., Amiro, B. and Munger, W.: Post field data quality control. In: Lee, X., Massman, W., Law, B. (Eds). Handbook of Micrometeorology, Kluwer Academic Pub, Dordrecht, Netherlands. pp. 181-208, 2004.

Grant, R.H. and Boehm, M.T.: Manure ammonia and hydrogen sulfide emissions from a western dairy storage basin. J. Environ. Qual. 44, 1-10, 2015.

Hendrix, P.F., Han, C.- R. and Groffman, P.M.: Soil respiration in conventional and no-tillage ecosystems under different winter cover crops. Soil Tillage Res. 12, 135-158, 1988.

Kaimal, J.C. and Finnigan, J.J.: Atmospheric Boundary Layer Flows: their structure and measurement. Oxford Univ. Press, NY, NY 289p, 1994.

Lee, X., Black, T.A., den Hartog, G, Neumann, H.H., Nesic, Z. and Olejnik, J.: Carbon dioxide exchange and nocturnal processes over a mixed deciduous forest. Agric. Forest Meteorol. 81, 13-29, 1996.

Lee, X., Finnigan, J. and Paw U, K.T.: Coordinate systems and flux bias error. In: Lee, X., Massman, W., Law, B. (Eds). Handbook of Micrometeorology, Kluwer Academic Pub, Dordrecht, Netherlands. pp 33-66, 2004.

Mahrt, L.: The near-calm stable boundary layer. Boundary Layer Meteorol. 140, 343-360, 2011.

Massman, W.J.: A review of the molecular diffusivities of H_2O, CO_2, CH_4, CO, O_3, SO_2, NH_3, N_2O, NO, and NO_2 in air, O_2 and N_2 near STP, Atmos. Environ. 32, 6, 111-1127, 1998.

Mosier, A, Shimel, D., Valentine, D., Bronson, K. and Parton, W.: Methane and nitrous oxide fluxes in native, fertilized and cultivated grasslands. Nature 350, 330-332, 1991.

Parkin, T.B. and Kaspar, T.C.: Nitrous oxide emissions from corn-soybean systems in the Midwest. J. Environ. Qual. 35, 1496-1506, 2006.

Parkin, T.B., Kaspar, T.C., Sennwo, Z., Prueger, J.H. and Hatfield, J.L.: Relationship of soil respiration to crop and landscape in the Walnut Creek watershed. J. Hydromet. 6, 812-824, 2005.

Pattey, E, Strachan, I.B., Desjardins, R.L. and Massheder, J.: Measuring CO_2 flux over terrestrial ecosystems using eddy covariance and nocturnal boundary layer methods. Agric. Forest Meteorol. 113, 145-158, 2002.

Pendall, E., Schwendenmann, L., Rahn, T., Millers, J.B. and Tans, P.P.: Land use and season affect fluxes of CO_2, CH_4, CO, N_2O, H_2 and isotopic source signatures in Panama: evidence from nocturnal boundary layer profiles. Global Change Biol. 16, 2721-2736, 2010.

Raich, J.W. and Tufekcioglu, A.: Vegetation and soil respiration: correlations and controls. Biogeochem. 48, 71-90, 2000.

Schaefer, K., Grant, R.H., Emeis, S., Raabe, A., von der Heide, C. and Schmid, H.P.: Areal-averaged trace gas emission rates from long-range open-path measurements in stable boundary layer. Atmos. Meas. Tech. 5, 1571-1583, 2012.

Tufekcioglu, A., Raich, J.W., Isenhart, T.M., Schultz, R.C.: Soil respiration within riparian buffers and adjacent fields. Plant Soil 229, 117-124, 2001.

USDA: Cropscape- Cropland Data Layer. Center for Spatial Information Science and Systems, National Agricultural Statistics Service, United States Department of Agriculture, https://nassgeodata.gmu.edu/CropScape/, (accessed 6/15/2017)

van de Wiel, B.J.H., Moene, A.F., De Ronde, W.H. and Jonker, H.J.J.: Local similarity in a stable boundary layer and mixing-length approaches: consistency of concepts. Boundary-Layer Meteorol. 128, 103-116, 2008.

Vesala, T., Kljun, N., Rannik, Ü., Rinne, J., Sogachev, A., Markkan, T., Sabelfeld, K., Foken, Th. and Lecelerc, M.Y.: Flux and concentration footprint modelling**:** State of the art. Envon. Poll. 152, 653-666, doi:10.1016/**j**.envpol.2007.06.070, 2007.

Venterea, R.T., Burger, M. and Spokas, K.A.: Nitrogen oxide and methane emissions under varying tillage and fertilizer management. J. Environ Qual. 34, 1467-1477, 2005.

Wagner-Riddle, C., Furon, A., McLaughlin, N.L., Lee, I., Barbeau, J., Jayasundrara, S., Parkin, G. and von Bertold, P.: Intensive measurement of nitrous oxide emissions from a corn-soybean-wheat rotation under two contrasting management systems over 5 years. Global Change Biol. 13, 1722-1736, 2007.

Xia, Y., Conen, F., Haszpra, L., Ferenczi, Z. and Zahorowski, W.: Evidence for nearly complete decoupling of very stable nocturnal boundary layer overland. Boundary-Layer Meteorol. 138, 163-170, 2011.

Table 1: 2015 Land use around the research site and literature-reported emissions for each land use.

Land use	1 km^2 area (%)[1]	10 km^2 area (%)[1]	CO_2 respiration ($\mu mol\ m^{-2}\ s^{-1}$)	Source	N_2O emissions (nmol $N_2O\ m^{-2}\ s^{-1}$)	Source
Maize production	83	47	Canopy:2.5-3.6	Pattey et al, 2002	0- 7.5 6.1-8.1	Eichner, 1990 Parkin and Kaspar, 2006
Soybean production	15	46	Soil/root: 2.9; Canopy: 3.6,4.3 Soil/root: 0.41,0.49 Canopy: 3.8 Canopy:2.5-7.5	Raich & Tufekcoglu, 1999; DeCosta, et al, 1986 Parkin et al, 2005 Pattey et al, 2002	0.3-1.2 1.7-2.0	Bemner et al, 1980 Parkin and Kaspar, 2006
Grass	2	2	Canopy: 3.5	Tufekcoglu,et al 2001	0.9-2.3	Eichner, 1990
Deciduous Forest	0	1	Soil/root: 2.2,2.5 Canopy: 5.2	Raich &Tufekcoglu, 1999 Lee at al, 1996	<0.3-0.6, 1.2	Bowden et al, 2000; Goodroad & Keeney, 1984
Bare ground	0	<1	Soil: 0.06,0.06,0.06	DeCosta, et al, 1986	1.4-2.0	Bremner et al, 1981
Alfalfa	0	<1	Canopy: 1.7 Soil/root: 1.1	DeCosta, et al, 1986	1.7-4.3	Duxbury and Bouldin, 1982

1: Land use during the 2015 growing season assessed using CropScape Cropland Data Layer (USDA,2017).

Table 2: Wind conditions over the maize canopy. Statistics based on 30-min averaging period of 10Hz 3D sonic anemometer measurements at indicated heights over the entire study period.

			8 m		5 m			8 m		
Time interval (LT)	**Flow condition at 8 m**	**Statistic**	**$U^{\dagger}$ (ms^{-1})**	**$z/\Lambda^{\ddagger}$**	**Friction velocity-u_* (ms^{-1})**	**Standard deviation of vertical velocity–σ_w (ms^{-1})**	**σ_w/u_***	**Friction velocity-u_* (ms^{-1})**	**Standard deviation of vertical velocity–σ_w (ms^{-1})**	**σ_w/u_***
1900-0300	Low turbulence u_*<=0.05 ms^{-1} n^{+}=290	Mean	1.05	16.05	0.04	0.003	0.066	0.02	0.002	0.080
		Standard deviation	0.45	0.80	0.02	0.003	0.152	0.01	0.002	0.176
	Turbulent u_*>0.05 ms^{-1} n=314	Mean	2.17	0.10	0.21	0.089	0.421	0.19	0.083	0.435
		Standard deviation	0.94	0.04	0.14	0.067	0.488	0.13	0.104	0.800
0300-0700	Low turbulence u_*<=0.05 ms^{-1} n=157	Mean	0.98	-3.43	0.04	0.003	0.072	0.03	0.002	0.086
		Standard deviation	0.44	0.32	0.02	0.004	0.204	0.01	0.004	0.322
	Turbulent u_*>0.05 ms^{-1} n=923	Mean	2.80	-1.33	0.36	0.212	0.593	0.33	0.200	0.605
		Standard deviation	1.45	0.00	0.17	0.188	1.090	0.17	0.171	1.021

†: U=wind speed

‡: Λ= Local Obukhov stability

+: n= number of 30-min measurements

Table 3: Characteristics of the nocturnal boundary layer at the top of the accumulation domain with stable conditions (positive local Obukhov length) at 8m. Statistics based on 30-min averaging periods.

Time interval (LT)	Flow condition at 8 m agl	6.3 m agl					
		Statistic	$\Delta T_s^{\dagger}/\Delta z$ ($^oC\ m^{-1}$)	$\Delta N_2O/\Delta z$ ($\mu mol\ m^{-4}$)	$\Delta CO_2/\Delta z$ ($mmol\ m^{-4}$)	$K^{\ddagger}_{N2O}$ ($m^2\ s^{-1}$)	K_{CO2} ($m^2\ s^{-1}$)
1900-0300	Low turbulence u_*^{+}<=0.05 ms^{-1}	Mean	-0.008	0.08	1.11	0.008	0.008
		Standard deviation	0.033	0.14	1.23	0.024	0.022
	Turbulent u_*>0.05 ms^{-1}	Mean	0.148	0.00	0.21	0.233	0.221
		Standard deviation	0.025	0.09	0.38	0.229	0.216
0300-0700	Low turbulence u_*<=0.05 ms^{-1}	Mean	0.005	0.06	0.82	0.010	0.009
		Standard deviation	0.053	0.09	0.96	0.111	0.105
	Turbulent u_*>0.05 ms^{-1}	Mean	0.270	0.00	0.02	0.601	0.568
		Standard deviation	0.035	0.19	0.18	0.307	0.290

+: u_* =friction velocity

†: T_s =sonic temperature

‡: K =diffusion coefficient

n

Table 4: Flux of N_2O and CO_2 across the top of the accumulation domain during stable (positive local Obukhov length) nocturnal conditions. Accumulation flux based on 90-min mass accumulations.

Flow condition at 8 m	Statistic	Gradient at top of domain (6.3 m agl)		N_2O accumulation flux ($nmol\ m^{-2}s^{-1}$)		CO_2 accumulation flux ($\mu mol\ m^{-2}s^{-1}$)	
		$\mu mol\ N_2O\ m^{-4}$	$mmol\ CO_2\ m^{-4}$	with or without measurable diffusion at 6.3 m	without measurable diffusion at 6.3 m	with or without measurable diffusion at 6.3 m	without measurable diffusion at 6.3 m
Low turbulence $u_*{}^{+}<=0.05\ ms^{-1}$	Mean	0.04	427	0.38	0.27	4.1	4.2
	SD‡	0.06	480	0.37	0.16	2.7	2.9
	n†	89	67	90	50	85	57
Turbulent $u_*>0.05\ ms^{-1}$	Mean	0.02	680	0.28	0.22	1.4	1.8
	SD	0.05	636	0.35	0.19	3.0	4.1
	n	59	59	60	40	106	53

+: u_*=friction velocity

‡: SD=standard deviation

†: n= number of 90-min values

Table 5: Comparative fluxes of N_2O and CO_2 based on the chamber and mass accumulation methods.

	Chamber flux			Mass accumulation flux			Ratio
Measurement period	n*	Mean	Standard deviation	n*	Mean	Standard deviation	Mass accumulation/ Chamber
CO_2	(#)	(μmol $m^{-2}s^{-1}$)	(μmol $m^{-2}s^{-1}$)	(#)	(μmol $m^{-2}s^{-1}$)	(μmol $m^{-2}s^{-1}$)	
23/7/15-31/7/15	-	-	-	36	1.48	0.46	-
1/8/15-22/8/15	55	1.30	0.80	96	0.84	0.44	0.6
23/8/14-2/9/15	11	0.21	0.08	21	0.18	0.13	0.9
N_2O	(#)	(nmol $m^{-2}s^{-1}$)	(nmol $m^{-2}s^{-1}$)	(#)	(nmol $m^{-2}s^{-1}$)	(nmol $m^{-2}s^{-1}$)	
23/7/15-31/7/15	18	1.56	0.81	36	1.74	0.35	1.1
1/8/15-22/8/15	52	2.09	1.30	96	1.02	0.34	0.5
23/8/14-2/9/15	25	0.40	0.17	21	0.38	0.21	1.0

*= number of measurements

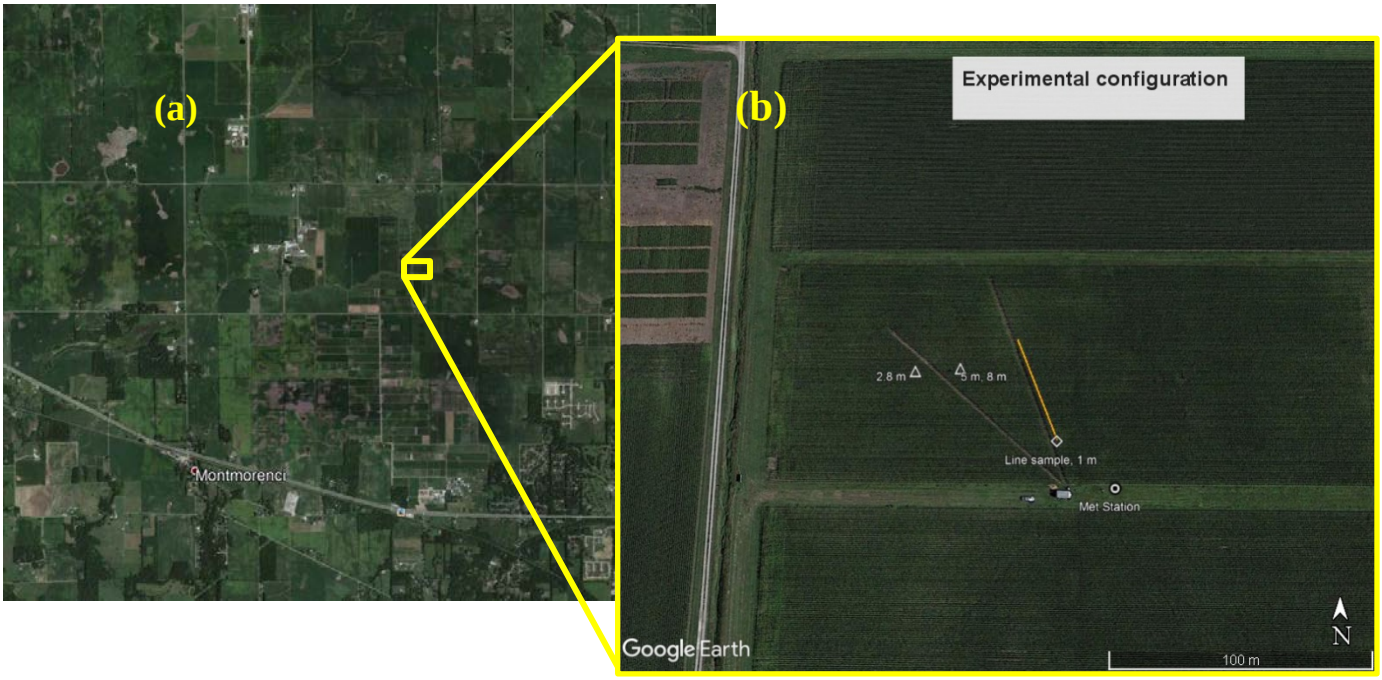

Figure 1: Experimental domain: GoogleEarth® images from August 2015 showing the homogeneous agricultural land use across the region surrounding the experimental field (40.495º latitude and -86.994º longitude: panel a) and the configuration of measurements in the experimental field (panel b). Locations and heights of the sonic anemometers and inlets (open triangles), integrated line sample (open diamond and orange line), and meteorological station (open circle) are indicated. Note scale in lower right corner.

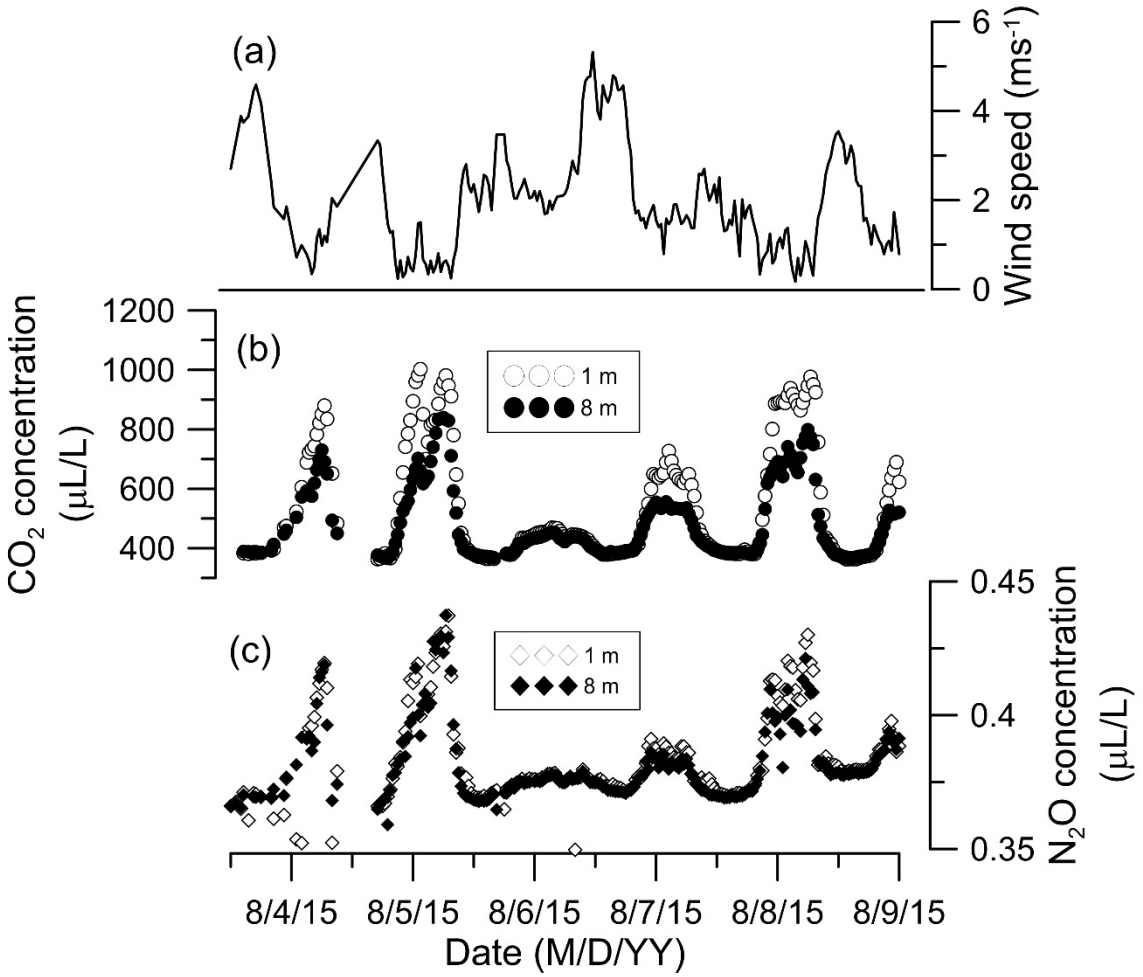

Figure 2: Changes in CO_2 and N_2O concentrations at the bottom and top of the measured domain relative to wind speed at 8 m. The wind speed at 8m (panel a, right ordinate), the CO_2 concentrations at 1 m and 8 m (panel b, left ordinate) and the N_2O concentrations at 1 m and 8 m (panel c, right ordinate) are indicated for a five-day period. Dates on the abscissa are indicated at the beginning of the indicated day (midnight). Note the increase in wind speed during the 8/5/15 night corresponds with a decrease in both the 1 m and 8 m concentrations of both CO_2 and N_2O. Date/time is local time.

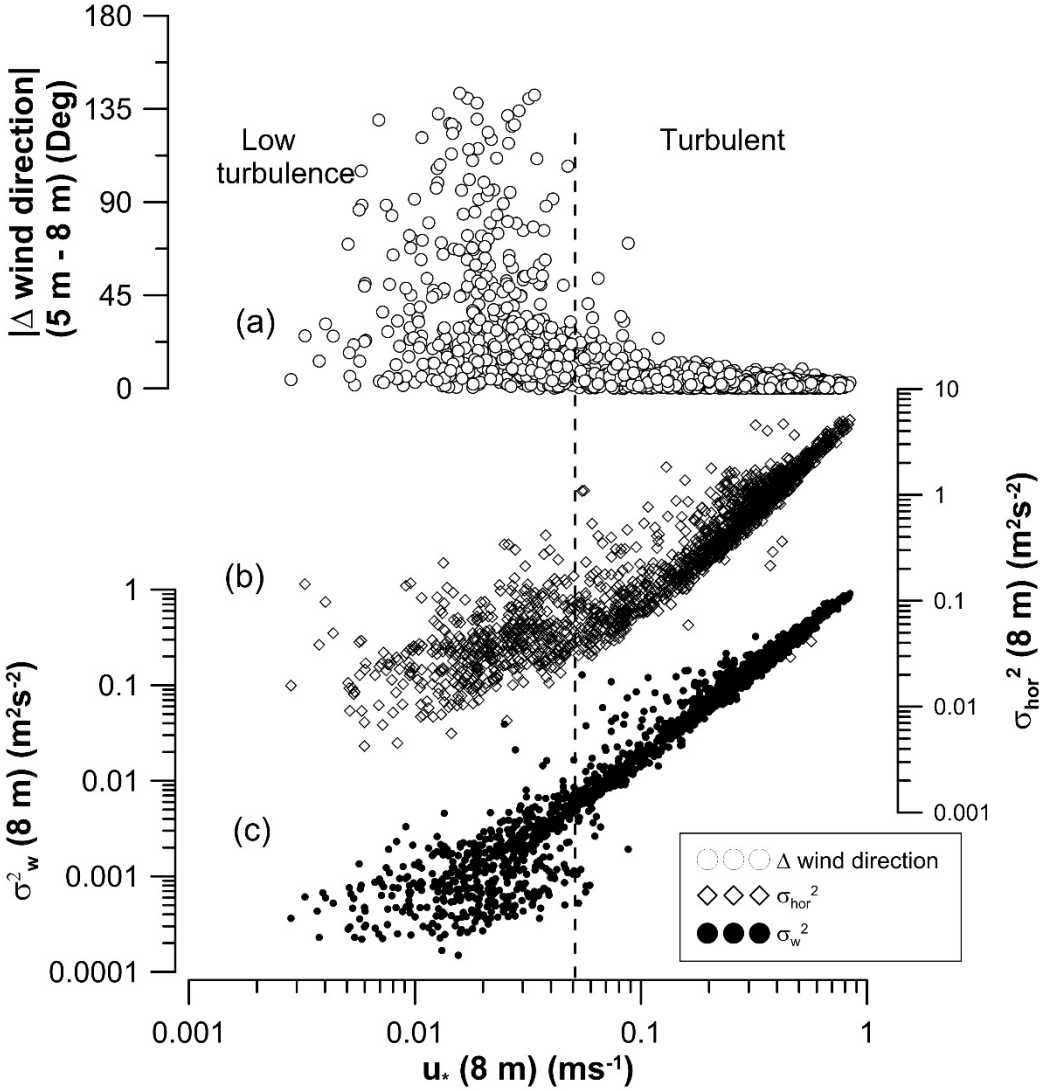

Figure 3: Wind conditions in the near-surface layer over the entire study period. The relationship between absolute value of change in wind direction (panel a with ordinate axis to left), horizontal wind velocity variance (σ_{hor}^2; panel b with ordinate axis to left) and the vertical wind velocity variance (σ_w^2; panel c with ordinate axis to right) with friction velocity (u_*) is indicated. The dashed line demarcates the separation of 'low turbulence' and 'turbulent' classifications for wind conditions. Note that the demarcation between 'low turbulence' and 'turbulent' flow corresponds with a σ_w^2 threshold of 0.01 m^2s^{-2}.

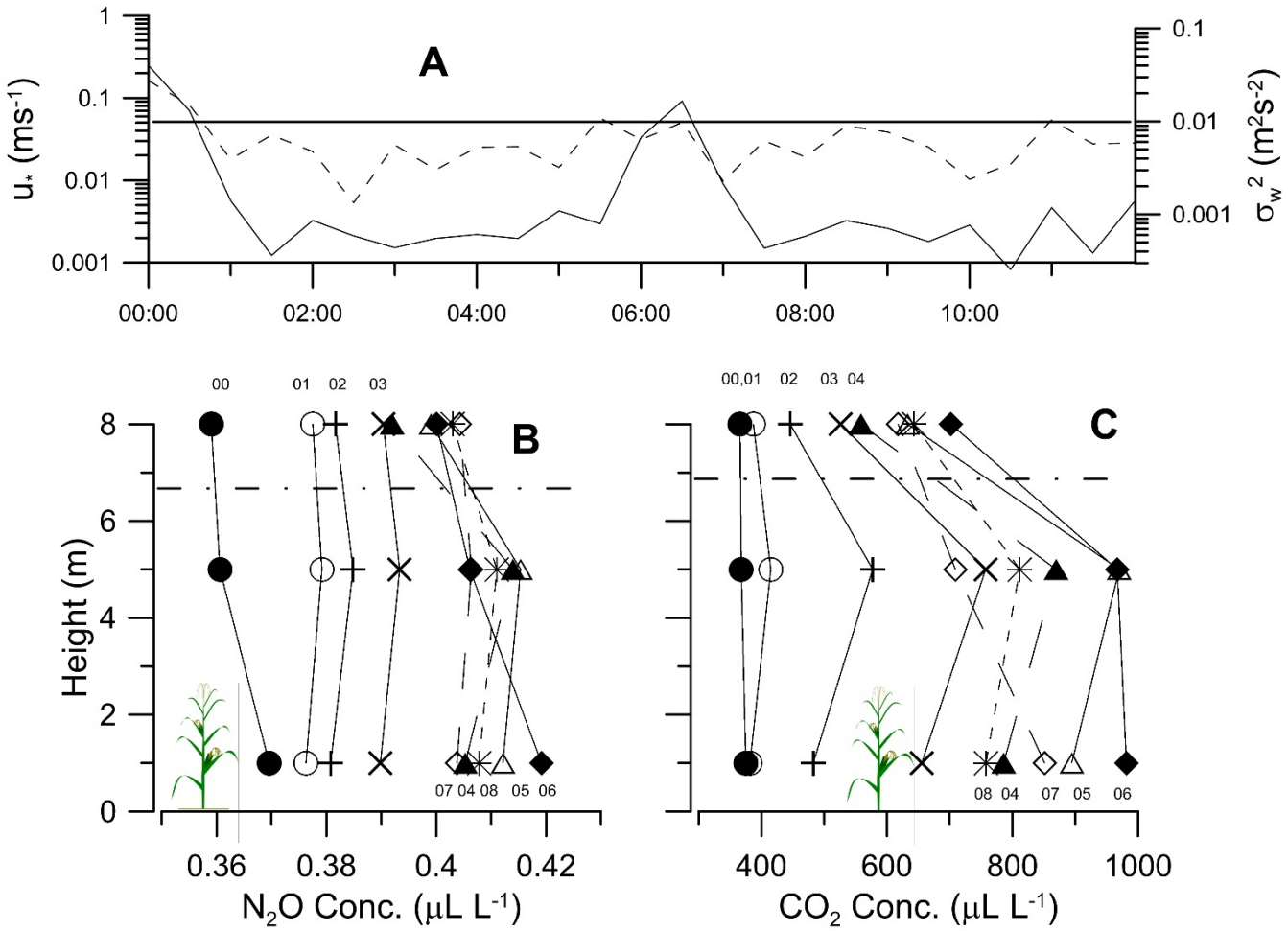

Figure 4: Near-surface atmospheric conditions during the night of 5 August, 2015. The friction velocity (u_*, left ordinate) and vertical wind velocity variance (σ_w^2, right ordinate) at 8 m are indicated from 1900 to 0700 LT in panel a. The solid line (panel a) indicates the upper thresholds for the 'low turbulence' classification. Labelled profiles (LT) of N_2O and CO_2 concentrations every hour from 1900 LT until 0300 LT are indicated with differing symbols and lines in panels b and c. Note the 0100-0200 LT burst of vertical wind variance (panel a) corresponds with losses in N_2O (panel b) and CO_2 (panel c). Sunrise and sunset times were 0649 and 2059 LT.

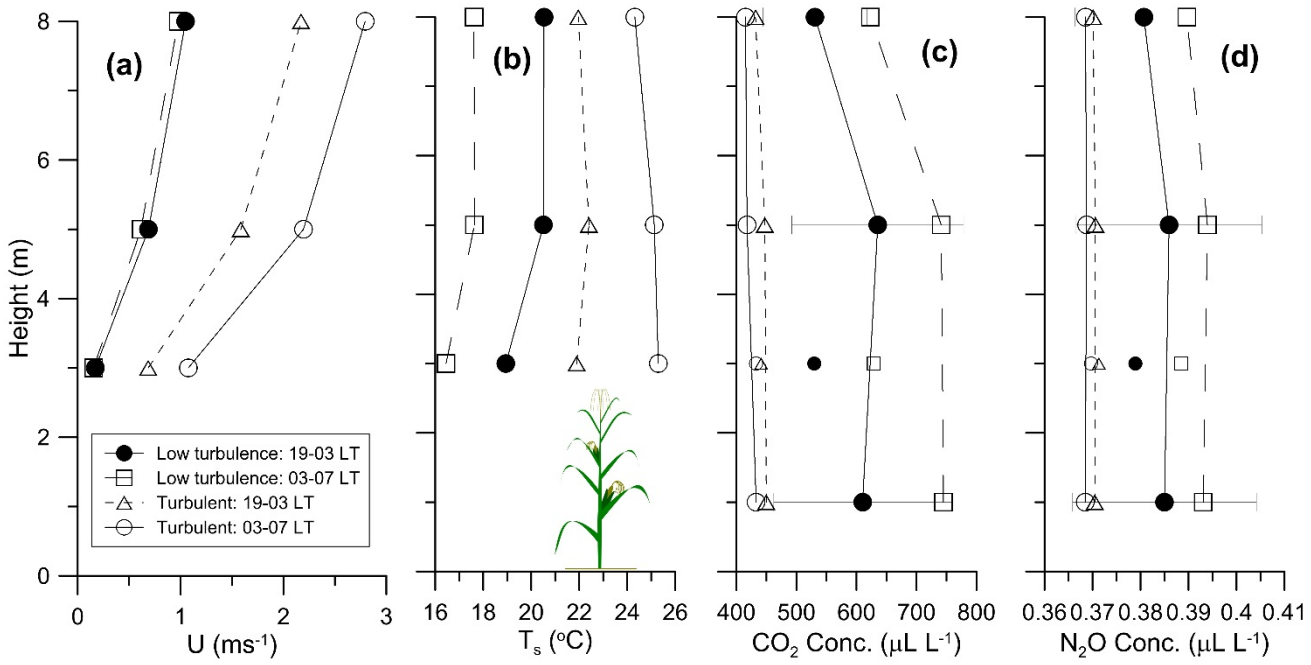

Figure 5: Mean profiles of wind speed, sonic temperature, and concentrations of CO_2 and N_2O under different friction velocity and time domain classes for the entire study period. The mean wind speed (U, panel a), sonic temperature (T_s; panel b), and concentration profiles of CO_2 (panel c) and N_2O (panel d) when the air at 8 m had low turbulence ($u_* < 0.05$ ms^{-1}) or turbulent ($u_* >= 0.05$ ms^{-1}) between 1900 and 0300 LT and 0300 and 0700 LT are indicated. Canopy height was 2.8 m. Smaller symbols not connected with lines represent concentration measurements excluded from mass accumulations due to their close proximity to the canopy top.

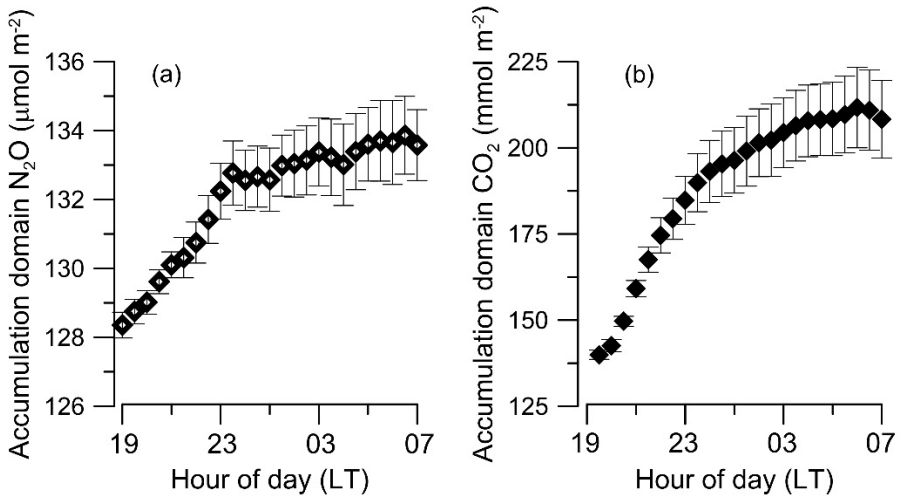

Figure 6: Accumulation of CO_2 and N_2O within the lowest 6.3m of the boundary layer during the night throughout the study period. The mean accumulations of N_2O (panel a) and CO_2 (panel b) are indicated with vertical error bars indicating the standard error of the mean of each 30-min mean accumulation. Sunrise is approximately 0600 to 0700 LT.

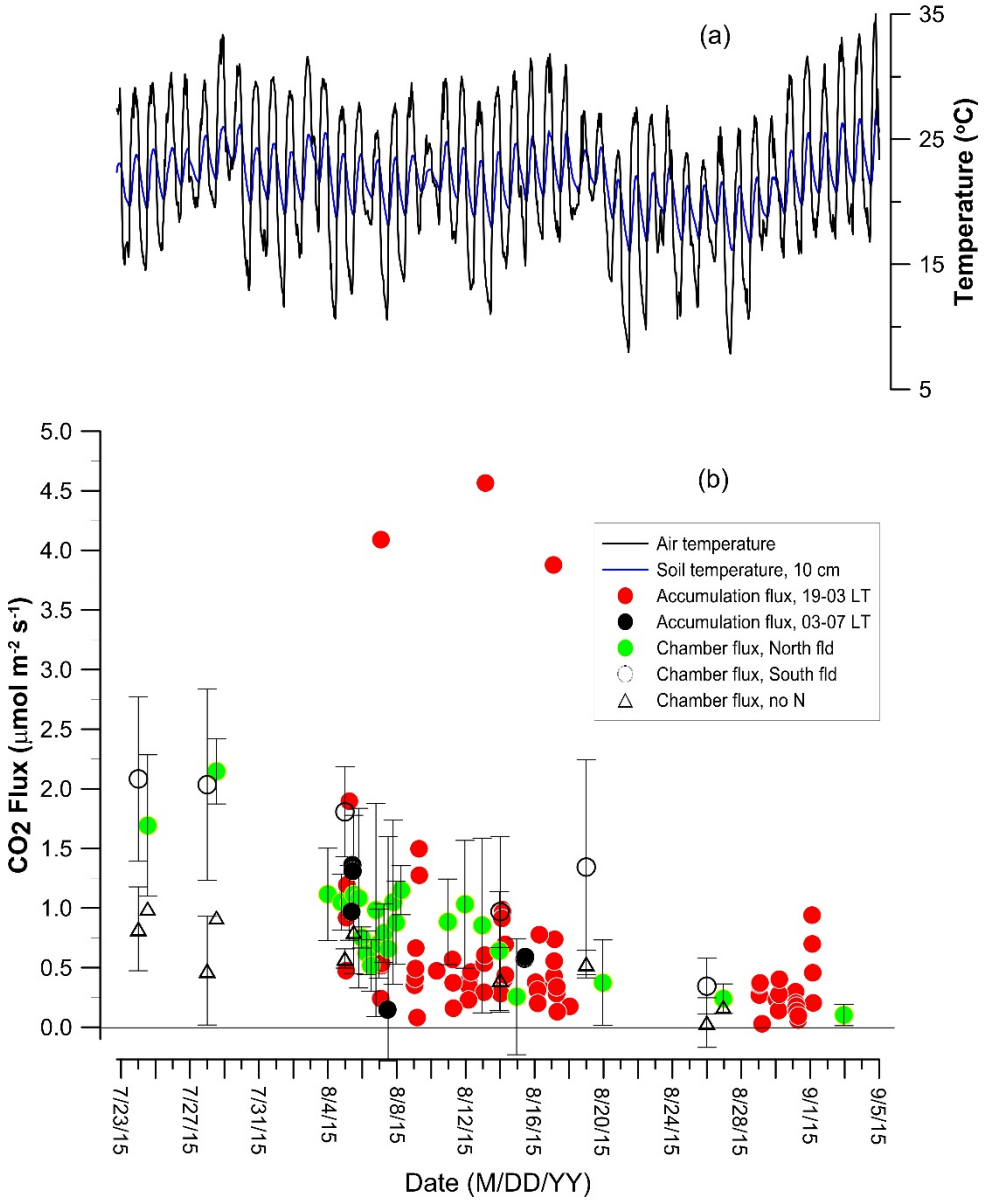

Figure 7: Temperatures and CO_2 flux based on accumulation and chamber methods. Diurnal variation in air (solid black line) and 10 cm soil at 10 cm depth (dashed blue line) during the period are indicated in panel a. Canopy fluxes calculated using accumulation method under stable, low turbulence conditions with or without measurable diffusion at 6.3 m and soil+root fluxes calculated using the chamber method from measurements made between 1000 and 1400 LT are indicated in panel b (ordinate axis with differing units to left and right). The standard deviation of the three chamber flux measurements in each field are indicated by the vertical bars.

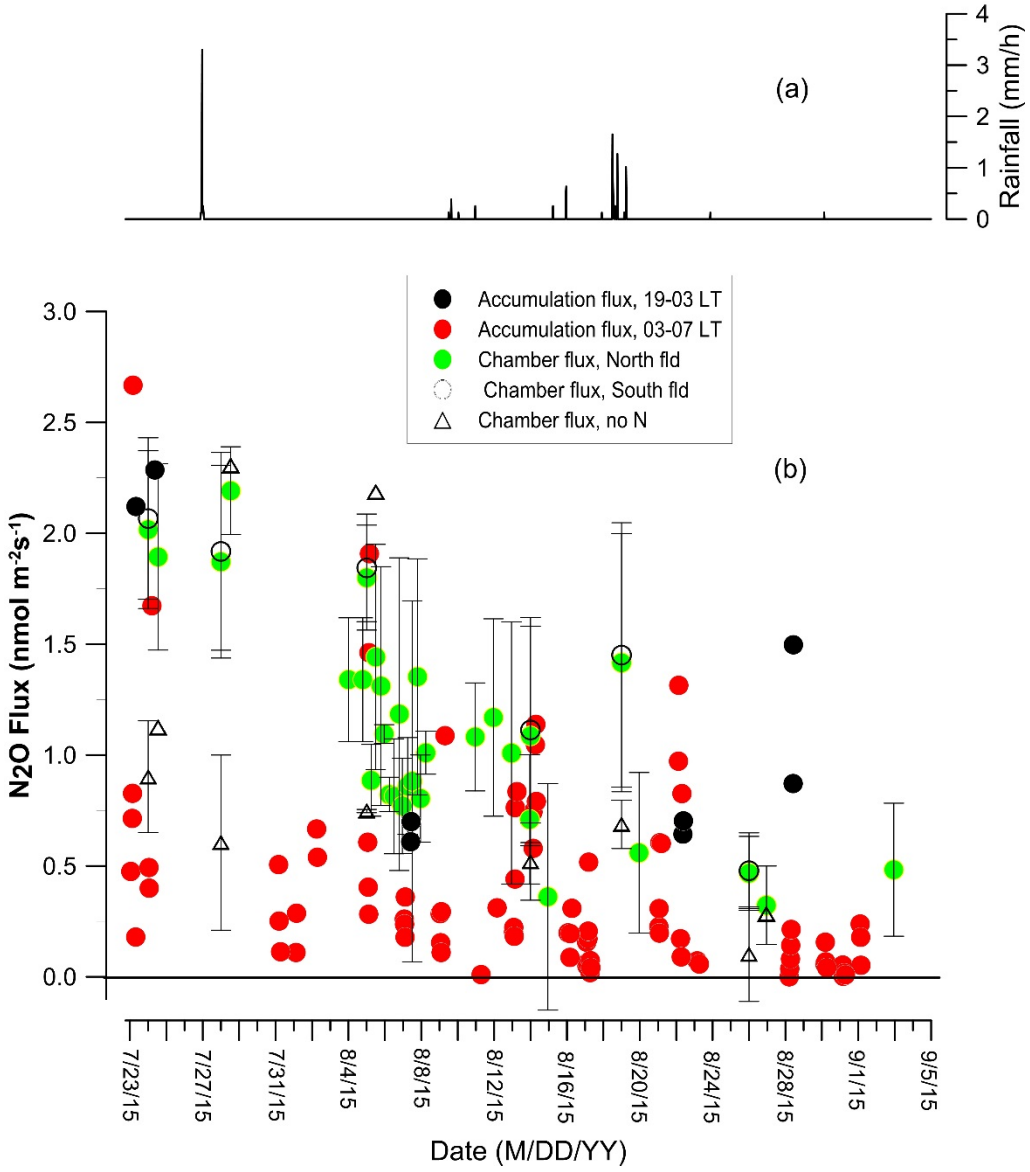

Figure 8: Precipitation and N_2O flux based on accumulation and chamber methods. Precipitation is indicated in panel a. Canopy fluxes calculated using accumulation method under stable, low turbulence conditions with or without measurable diffusion at 6.3 m and soil+root fluxes calculated using the chamber method from measurements made between 1000 and 1400 LT are indicated in panel b (ordinate axis with differing units to left and right). The standard deviation of the three chamber flux measurements in each field are indicated by the vertical bars.